RESEARCH PAPER

Molecular Hybridization of Quinoline-2-one and 1,2,3-Triazole: Design, Synthesis, and Cytotoxic Activity Against Pancreatic Cancer Cells

Deepak Bokka[1], Priya[1], Pasupala Pavan[3], Anupama Sharma[2*], Mallappa[1], Neeraj Kumar[1], Mukesh Jangir[1], Girish Chandra Sharma[1*]

[1]Department of Applied Sciences (Chemistry), NIET, Nims University Rajasthan, Jaipur, 303121.

Deepak.biocon@gmail.com ,priya@nimsuniversity.org , Mallappa.naikodi@nimsuniversity.org ,Neeraj.kumar1@nimsuniversity.org , Mukesh.kumari@nimsuniversity.org ,Girishchandra.sharma@nimsuniversity.org

[2]Research and Innovation Cell, Nims University Rajasthan, Jaipur 303121.

Anupama.sharma@nimsuniversity.org

[3]Department of Humanities and Basic Sciences, G. Pulla Reddy Engineering College, Kurnool, Andhra Pradesh,518007

Pavan.pasupala@gmail.com

*Corresponding author: Anupama Sharma / Girish Chandra Sharma

Received: 5th May, 2026; Revised: 23th May, 2026; Accepted: 13th June, 2026; Available Online: 17th June, 2026

ABSTRACT

A novel series of 1,2,3-triazole-linked quinolin-2-one derivatives, specifically 2-(5-{[(2-oxo-1,2,3,4-tetrahydroquinolin-6-yl)oxy]methyl}-1H-1,2,3-triazol-1-yl)-N-phenylacetamide analogues, were designed and synthesized through a highly efficient copper-catalyzed azide-alkyne cycloaddition (CuAAC) reaction, which is known as the click reaction. This key step coupled a 6-propargyloxy-tetrahydroquinolinone scaffold with diverse 2-azido-N-phenylacetamide derivatives, yielding the target hybrids in good to excellent yields (75-88%). The structures of all final compounds (8-12) were rigorously confirmed using comprehensive spectroscopic techniques. ^{1}H and ^{13}C NMR spectra unambiguously verified the formation of the 1,4-disubstituted triazole ring, the methylene linkers, and the integrity of both pharmacophores, while high-resolution mass spectrometry (HRMS) data confirmed the exact molecular mass of each compound with high precision. The in vitro anticancer potential of the library was evaluated against MiaPaCa2 human pancreatic cancer cells using a standardized MTT assay after a 48-hour incubation period, with gemcitabine as the positive control. All compounds exhibited dose-dependent cytotoxic activity, establishing a clear structure-activity relationship (SAR). Compound 8, bearing an unsubstituted phenyl ring, was the most potent (IC_{50} = 28.22 µM). Halogenation at the ortho (9, IC_{50} = 32.33 µM) or meta (10, IC_{50} = 46.32 µM) position reduced activity, while dichloro (11) and methoxy (12) substituents led to a significant drop in potency. Although the series was less active than gemcitabine (IC_{50} = 4.55 µM), the study successfully validates the triazole-quinolinone molecular hybrid as a promising scaffold, identifying compound 8 as a viable lead for future optimization campaigns aimed at enhancing anticancer efficacy.

Keywords: 1,2,3-Triazole; Click Chemistry; CuAAC; Quinolin-2-one; Anticancer Activity; Cytotoxicity; Structure-Activity Relationship.

How to cite this article: Bokka D, Priya, Pavan P, Sharma A, Mallappa, Kumar N, Jangir M, Sharma GC. Molecular Hybridization of Quinoline-2-one and 1,2,3-Triazole: Design, Synthesis, and Cytotoxic Activity Against Pancreatic Cancer Cells. Int J Drug Deliv Technol. 2026;16(63s):1506-1520. DOI: 10.25258/ijddt.16.63s.152

1. Introduction:

The five-membered heterocycle 1,2,3-triazole is a cornerstone of contemporary medicinal chemistry, valued for its metabolic stability, strong dipole moment, and capacity to participate in key non-covalent interactions, such as hydrogen bonding, which mimic biological motifs like peptide bonds [1,2]. Its significance is deeply connected to the development of the copper-catalyzed azide-alkyne cycloaddition (CuAAC), a quintessential "click chemistry" reaction renowned for its high yield,

selectivity, and functional group tolerance under mild, often aqueous conditions [3,4]. The CuAAC reaction has transformed the 1,2,3-triazole from a synthetic target into a readily accessible, indispensable pharmacophore, enabling its widespread incorporation into drug discovery campaigns [5]. As a privileged scaffold, triazole derivatives exhibit a broad spectrum of bioactivities, including anticancer effects mediated through mechanisms like kinase inhibition and tubulin disruption, as well as notable antimicrobial properties [6–9].

Similarly, the quinolin-2-one (carbostyril) nucleus represents another privileged scaffold in drug design, recognized for its diverse pharmacological profile encompassing anticancer, antimicrobial, and anti-inflammatory activities [10,11]. Its planar aromatic system facilitates interactions with biological targets via intercalation or π-stacking, while the lactam moiety and variable substitution patterns allow for fine-tuning of activity and drug-like properties [12]. Several quinolinone-based compounds have demonstrated promising anticancer potential by targeting topoisomerases, modulating kinase signaling, and inducing apoptotic pathways [13,14].

The strategy of molecular hybridization, which combines two or more bioactive pharmacophores into a single entity to improve efficacy or achieve dual mechanisms of action, is a well-established approach in rational drug design [15]. The fusion of the 1,2,3-triazole and quinolin-2-one scaffolds via the robust CuAAC linkage presents a logical path to create novel chemical entities with potentially enhanced or synergistic biological profiles [16]. Previous studies on triazole-linked quinoline/quinolinone hybrids have reported improved anticancer and antimicrobial activities compared to their parent fragments, validating this design rationale [17,18].

In continuation of our research toward novel anticancer agents and inspired by the potential of molecular hybridization, we herein report the design, synthesis, and biological evaluation of a new series of 1,2,3-triazole-linked quinolin-2-one derivatives. The synthetic approach employs the reliable CuAAC reaction to conjugate a 6-propargyloxy-tetrahydroquinolin-2-one alkyne with a panel of 2-azido-N-(substituted-phenyl)acetamide derivatives. All final hybrids (8-12) were thoroughly characterized by modern spectroscopic and spectrometric techniques (^{1}H NMR, ^{13}C NMR, and HRMS). Furthermore, their in vitro cytotoxic potential was evaluated against the human pancreatic cancer cell line MiaPaCa2 to establish preliminary structure-activity relationships (SAR) and identify a lead compound for future development.

2. Materials and Methods

2.1. Materials

All chemicals and solvents were of analytical or laboratory reagent grade. Starting materials and reagents including p-anisidine, aniline, 2-chloroaniline, 3-chloroaniline, 3,4-dichloroaniline, 3-chloropropanoyl chloride, chloroacetyl chloride, propargyl bromide (80% w/w in toluene, Caution: lachrymator), sodium azide (Caution: toxic), sodium borohydride, sodium ascorbate, copper(II) sulfate pentahydrate, anhydrous aluminum chloride, anhydrous sodium carbonate (Na_2CO_3), anhydrous potassium carbonate, and anhydrous sodium sulfate—were purchased from Sigma-Aldrich, Merck, or HiMedia and were used as received. All solvents like toluene, N,N-dimethylacetamide (DMA), N,N-dimethylformamide (DMF), acetone, dichloromethane (DCM), ethyl acetate (EtOAc), n-hexane, n-butanol, methanol (MeOH), and diethyl ether (Et_2O) were purified and dried prior to use following standard laboratory protocols. Toluene and DMF were dried over activated molecular sieves (4 Å), while DCM and Et_2O were distilled over calcium hydride.

2.2. General Methods and Instrumentation

Reaction progress was monitored by analytical thin-layer chromatography (TLC) on pre-coated silica gel 60 F_{254} aluminum plates (Merck). Spots were visualized under ultraviolet light (λ = 254 nm and 365 nm) and by charring after treatment with an appropriate staining solution (e.g., vanillin/sulfuric acid or potassium permanganate). Melting points were determined in open glass capillaries using a Büchi M-560 melting point apparatus and are reported as uncorrected values. Fourier-transform infrared (FT-IR) spectra were recorded on a PerkinElmer Spectrum Two spectrophotometer equipped with a universal ATR accessory. Spectra were acquired in the range of 4000–400 cm^{-1} at a resolution of 4 cm^{-1} with 16 scans per sample. Nuclear magnetic resonance (NMR) spectra were acquired at 25 °C on a Bruker Avance NEO spectrometer operating at 400 MHz for ^{1}H and

101 MHz for ^{13}C nuclei, using deuterated dimethyl sulfoxide (DMSO-d_6) as the solvent. Chemical shifts (δ) are reported in parts per million (ppm) relative to the residual solvent peak (DMSO-d_6: δH 2.50 ppm, δC 39.52 ppm) as an internal reference. Coupling constants (J) are reported in Hertz (Hz).

2.2.1. Synthesis of N-(4-methoxyphenyl)-3-chloropropionamide (Compound 2)

A three-necked round-bottom flask (3 L) equipped with a dropping funnel and a thermometer was charged with p-anisidine (1) (200 g, 1.62 mol), $NaHCO_3$ (205 g, 2.44 mol), and toluene (400 mL). A separate solution of 3-chloropropionyl chloride (207.5 g, 1.63 mol) in toluene (400 mL) was prepared and added dropwise to the vigorously stirred suspension over 1.5 hours, during which the internal temperature was maintained at 50 °C. Following the addition, the reaction mixture was heated to 60 °C and stirred for an additional hour, with reaction progress monitored by thin-layer chromatography (TLC). After cooling to ambient temperature, the mixture was carefully acidified by the slow addition of a 10% (v/v) aqueous hydrochloric acid solution (prepared from 100 mL of concentrated HCl diluted with 900 mL of water) over 30 minutes. The resulting biphasic mixture was filtered, and the collected solid residue was washed sequentially with water (500 mL) and toluene (250 mL). The crude product was subsequently dried overnight in an oven at 60 °C to afford 334 g of N-(4-methoxyphenyl)-3-chloropropionamide as an off-white crystalline solid as shown in scheme 1. This mass corresponds to a moderate yield of 86.6%, calculated from the limiting reagent, p-anisidine (theoretical yield: 385.6 g).

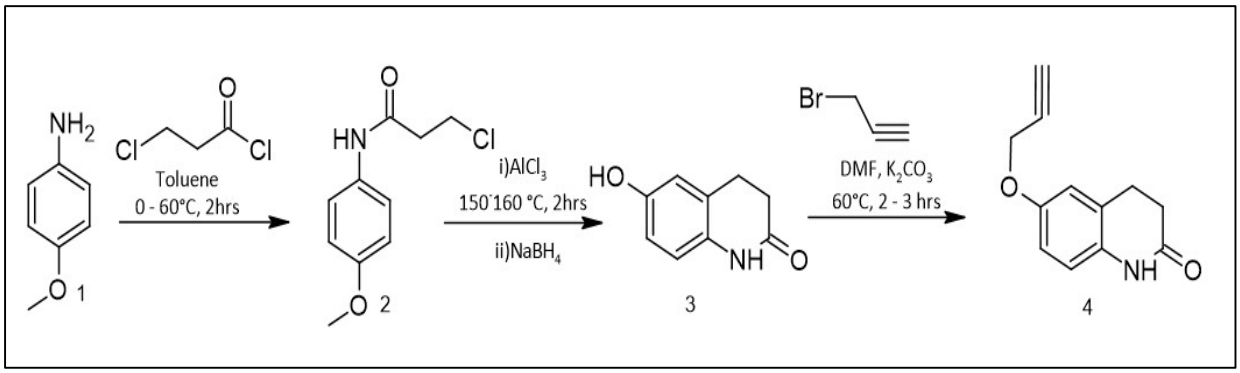

Scheme 1: Stepwise synthetic route for the preparation of key intermediates 2, 3, and 4, illustrating the specific reagents and conditions employed in each transformation.

2.2.2 Synthesis of 6-hydroxy-3,4-dihydroquinolinone (Compound 3)

A three-necked round-bottom flask (3 L), equipped with a mechanical stirrer and a thermometer, was charged with N-(4-methoxyphenyl) -3-chloropropionamide (300 g, 1.40 mol) and N,N-dimethylacetamide (165 mL, 1.82 mol). To this mixture, aluminum trichloride $AlCl_3$ (760 g, 5.70 mol) was added portion-wise with vigorous stirring over a period of 2 hours. The addition was exothermic, causing the internal temperature to rise from approximately 25 °C to 140 °C. The resulting slightly cloudy, colorless solution was then heated to 150–160 °C and maintained at this temperature with stirring for 2 hours, during which the mixture transformed into a stirrable slurry. After cooling to ambient temperature, the reaction mass was carefully quenched by pouring it into ice-cold water (5.5 L) in a fume hood equipped with an acid-gas trap to absorb evolved hydrogen chloride. Sodium borohydride (30 g, 0.79 mol) was then added in portions to the quenched mixture, resulting in a color change from gray to off-white. The mixture was stirred for an additional 30 minutes at room temperature and then filtered. The collected solid was washed thoroughly with water (2 L) and dried overnight in a vacuum oven at 60 °C to afford 212 g of 6-hydroxy-3,4-dihydroquinolin-2(1H)-one as a light-colored solid as depicted in scheme 1. The yield was 84.5 %, calculated from the limiting reagent N-(4-methoxyphenyl) -3-chloropropionamide (theoretical yield: 250.8 g).

2.2.3. Synthesis for the 6-(prop-2-yn-1-yloxy)-3,4-dihydroquinolin-2(1H)-one (Compound 4)

A round-bottom flask equipped with a magnetic stir bar was charged with 6-hydroxy-3,4-dihydroquinolin-2(1H)-one (0.050 mol, 8.91 g) and anhydrous N,N-dimethylformamide (DMF, 150 mL). To this stirring suspension, anhydrous potassium carbonate (K_2CO_3, 0.100 mol, 13.82 g,) was added. After stirring for 5 minutes, propargyl bromide (0.055 mol, 80% w/w in toluene, ~6.5 mL, 1.1 equiv) was introduced dropwise over 10 minutes. The resulting mixture was heated to 60 °C and stirred vigorously for 4 hours, with the reaction progress monitored by thin-layer chromatography (TLC). Upon completion, the reaction mixture was cooled and carefully poured into a beaker containing crushed ice (ca. 300 g) with stirring. The aqueous mixture was extracted with dichloromethane (2 × 150 mL). The combined organic extracts were dried over anhydrous sodium sulfate (Na_2SO_4), filtered, and concentrated under reduced pressure to afford the crude product. Purification by recrystallization from a suitable solvent (e.g., ethyl acetate/hexane) yielded Compound 4 as a solid (scheme 1).

Key Notes for the Procedure:

- The use of anhydrous K_2CO_3 and DMF is crucial for the efficient O-alkylation of the phenolic hydroxyl group.
- The propargyl moiety introduced in this step provides an alkyne functional group for subsequent copper-catalyzed azide-alkyne cycloaddition (CuAAC) “click chemistry”.

2.2.4 Synthesis of 2-chloro-*N*-phenylacetamide (Compound 6)

To a stirred solution of the substituted aniline (5) in dry acetone, chloroacetyl chloride (1.0 equiv) was added dropwise at room temperature. The reaction mixture was stirred for 15 minutes, after which it was carefully poured onto crushed ice. The resulting precipitate was collected by vacuum filtration, washed thoroughly with cold water, and dried under reduced pressure. The crude N-substituted-2-chloroacetamide intermediate was obtained as a solid as shown in scheme 2 and used directly in the subsequent step without further purification.

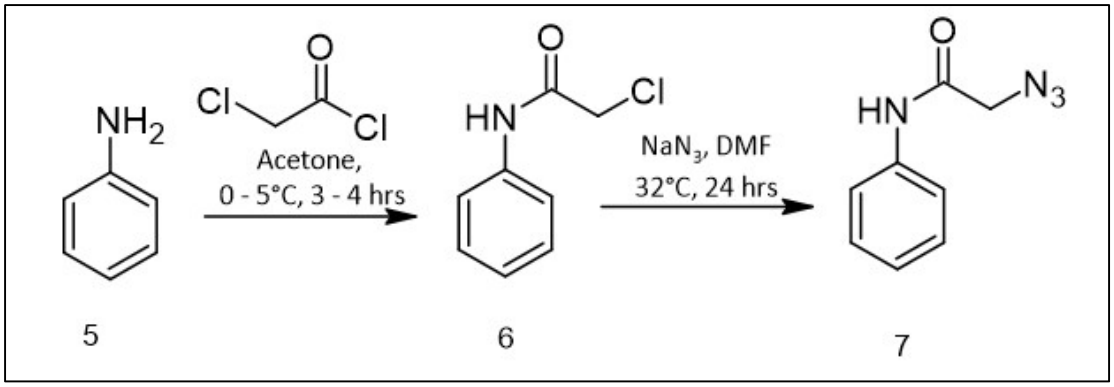

Scheme 2: Stepwise synthetic route for the preparation of key intermediates 6 and 7 with the starting material 6, illustrating the specific reagents and conditions employed in each transformation.

2.2.5 Synthesis of 2-azido-*N*-phenylacetamide (Compound 7)

A round-bottom flask equipped with a magnetic stir bar was charged with intermediate INT-4 (1.0 equiv) in anhydrous N,N-dimethylformamide. To this solution, sodium azide (NaN_3, 3.0 equiv) was added in a single portion. The reaction mixture was stirred vigorously at room temperature for 24 hours.Upon completion (monitored by TLC), the mixture was carefully poured onto crushed ice (~200 g) with stirring. The precipitated solid was collected by vacuum filtration, washed thoroughly with cold water, and dried under reduced pressure to afford the corresponding organic azide derivative as a solid (scheme 2).

Key Notes:

- This transformation proceeds via a nucleophilic substitution (SN_2) to convert a halide or other suitable leaving group in INT-4 into an azide functionality.
- The use of a polar aprotic solvent (DMF) facilitates the reaction. Appropriate safety precautions must be observed when handling organic azides.

2.2.6. Synthesis of 2-(5-{[(2-oxo-1,2,3,4-tetrahydroquinolin-6-yl)oxy]methyl}-1*H*-1,2,3-triazol-1-yl)-*N*-phenylacetamide (Compound 8)

To a round-bottom flask equipped with a magnetic stir bar was added a solvent mixture of N,N-dimethylformamide (DMF), water, and n-butanol (1:1:1 v/v/v).To this solvent system, the organic azide INT-3 (1.0 equiv) and the alkyne-functionalized intermediate INT-5 (1.0 equiv) were added sequentially at room temperature. Catalytic amounts of sodium ascorbate (0.2 equiv) and copper(II) sulfate pentahydrate (0.1 equiv) were added to the stirring solution, initiating the characteristic copper-catalyzed azide-alkyne cycloaddition (CuAAC) click' reaction. The resulting heterogeneous mixture was stirred vigorously at room temperature for 24 hours.

Upon completion (as monitored by TLC), the reaction mixture was poured onto crushed ice (~300 g) to precipitate the crude 1,2,3-triazole product. The solid was collected by vacuum filtration and subsequently stirred with a dilute aqueous ammonia solution (e.g., 2-5% v/v) for 30 minutes at room temperature to chelate and remove residual copper catalyst. The purified solid was isolated by a second filtration, washed thoroughly with water, and dried under reduced pressure to afford the final 1,2,3-triazole conjugate as a solid. This step constitutes the key 'click' cycloaddition, constructing the 1,2,3-triazole ring—a privileged pharmacophore (scheme 3). The ternary solvent system is employed to ensure homogeneity and facilitate the reaction between organic azide and alkyne precursors. The post-reaction ammonia wash is a critical purification step that removes copper impurities, which are essential for subsequent biological evaluation.

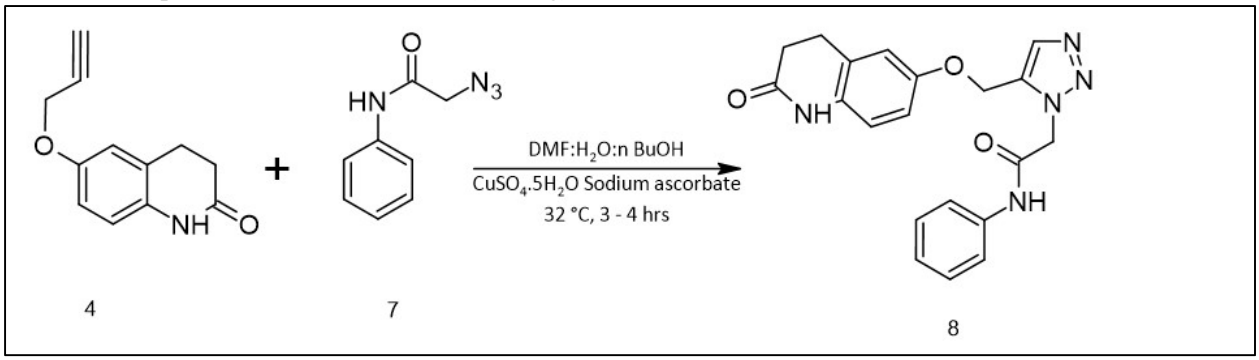

Scheme 3: synthetic route for the preparation of compound 8, illustrating the specific reagents and conditions employed in the transformation.

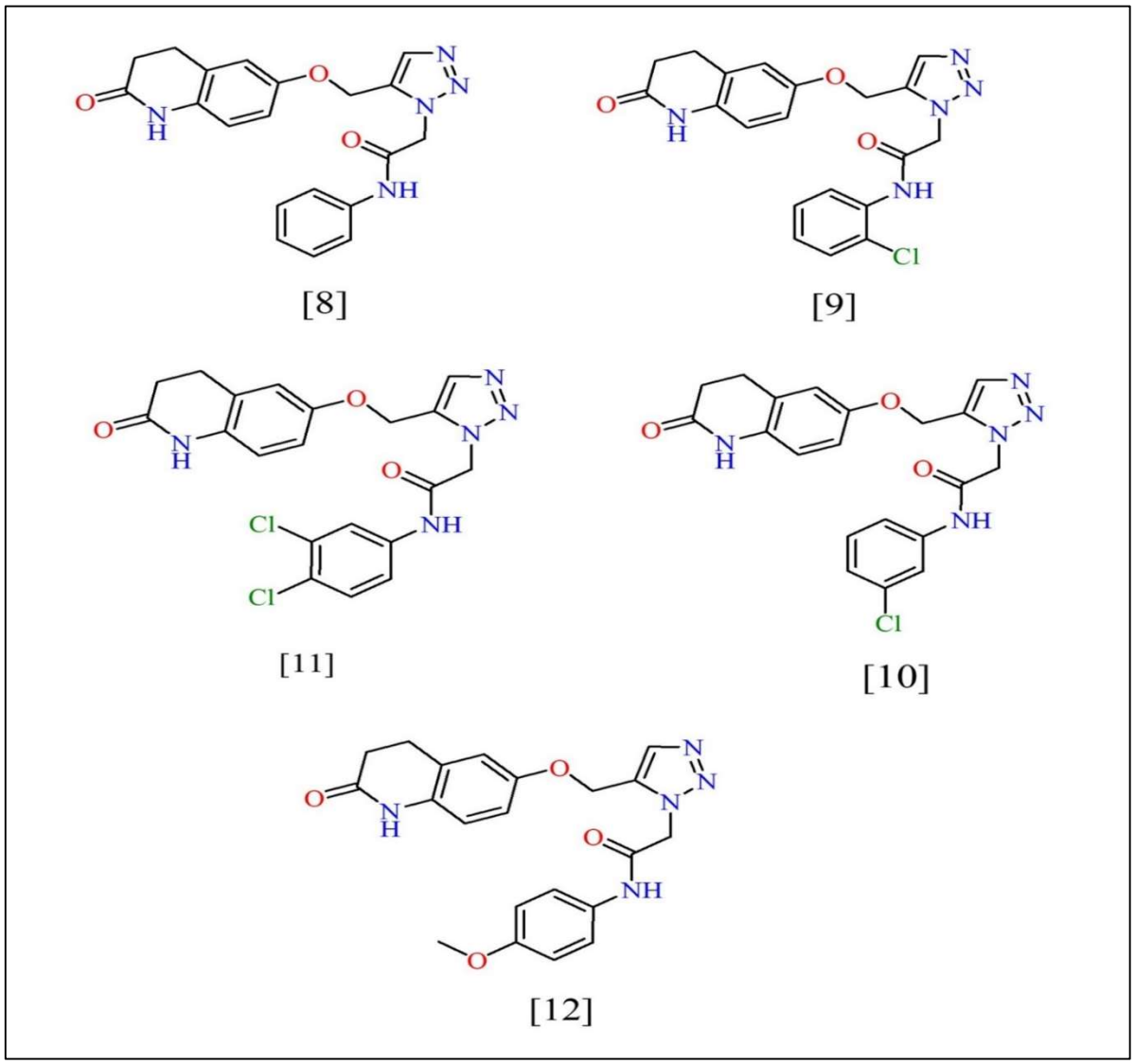

Figure 1: Structure of the synthesized compounds 8-12.

3. Results and Discussion:

3.1 NMR spectroscopy

The ^{1}H NMR spectra (DMSO-d6, 400 MHz) of Compounds 8-12 consistently display the characteristic signals of the shared 2-oxo-1,2,3,4-tetrahydroquinoline and 1,2,3-triazolylacetamide core [19,20]. The aliphatic methylene's of the dihydroquinoline ring appear as triplets near δ 2.40 ppm (2H, CH_2C=O) and δ 2.83 ppm (2H, CH_2Ar) [21]. Two distinct singlet methylene linkers are present: the O–CH_2–triazole proton resonance is consistently at ~δ 5.10 ppm (2H, s), while the N–CH_2–C=O protons resonate between δ 5.34-5.45 ppm (2H, s), showing slight variation with the aniline substituent [22]. The aromatic region for the tetrahydroquinoline moiety shows a typical pattern of two doublets and one singlet between δ 6.76-6.90 ppm [23]. The triazole ring's C-5 proton is a clear singlet at ~δ 8.22 ppm [24]. Two exchangeable amide NH singlets are observed: the lactam NH is consistently near δ 9.93-9.94 ppm, while the anilide NH signal varies more significantly (δ 10.09-10.80 ppm), influenced by the substitution on the phenyl ring [25]. The signals for the N-aryl ring differ distinctively for each compound: Compound 8 (phenyl) shows a simple AA'XX' pattern; Compound 9 (2-Cl-phenyl) exhibits a complex multiplet pattern characteristic of ortho-substitution [26]; Compound 10 (3-Cl-phenyl) shows a distinct singlet and doublets; Compound 11 (3,4-diCl-phenyl) displays two doublets and a singlet; and Compound 12

(4-OCH_3-phenyl) presents a pair of symmetric doublets along with a sharp methoxy singlet at δ 3.70 ppm [27].

The expected ^{13}C NMR spectra for this series would show approximately 20-21 distinct signals, reflecting the common scaffold and specific aryl substitutions [28]. Key features across all compounds would include the lactam carbonyl at ~δ 170-172 ppm and the acetamide carbonyl at ~δ 165-167 ppm [29]. The aromatic region (δ 110-155 ppm) would contain signals for the tetrahydroquinoline ring and the substituted aniline ring, with patterns and chemical shifts diagnostically altered by the substituents (e.g., electron-withdrawing chlorine atoms deshield ortho/para carbons, while the methoxy group in Compound 12 strongly shields its ortho and para carbons and deshields the ipso carbon) [30]. The methylene linker carbons (O–CH_2 and N–CH_2) are expected in the range of δ 52-62 ppm. The aliphatic methylenes of the tetrahydroquinoline core would appear near δ 25 ppm (CH_2C=O) and δ 35 ppm (CH_2Ar). For Compound 12, an additional signal from the methoxy group would be present at ~δ 55.5 ppm.

3.2 Mass spectrometry

High-Resolution Mass Spectrometry (HRMS) in EI^+ mode confirmed the molecular formulas of all synthesized compounds. Compound 8 ($C_{20}H_{19}N_5O_3$) showed an $[M]^+$ peak at m/z 377.39. The chlorinated analogues Compound 9 and Compound 10 (both $C_{20}H_{18}ClN_5O_3$) displayed the expected $[M]^+$ ion at m/z 411.8, each with the characteristic isotopic signature of a single chlorine atom [19-20]. Compound 11 ($C_{20}H_{17}Cl_2N_5O_3$) exhibited its $[M]^+$ peak at m/z 446.28, matching the calculated mass and showing the distinctive isotopic cluster pattern for two chlorine atoms [21]. Compound 12 ($C_{21}H_{21}N_5O_4$) showed an $[M]^+$ ion at m/z 407.42. In all cases, the observed exact mass matched the calculated value for the proposed molecular formula, providing definitive confirmation of the synthesized structures [22].

3.3 Spectral Data

3.3.1 2-(5-{[(2-oxo-1,2,3,4- tetrahydroquinolin-6-yl)oxy]methyl}-1*H*-1,2,3-triazol-1-yl)-*N*-phenylacetamide (Compound 8)

^1H NMR(DMSO-d6,ppm,400MHz) 2.38-2.42(2H,t,CH2),2.81-2.85(2H,t,CH2), 5.1(2H,S,CH2), 5.34(2H,S,CH2),6.78-6.82(2H,d,CH),6.9(1H,S,CH),7.06-7.10(1H,m,CH), 7.31-7.35(2H,t,CH) ,7.56-7.58(2H,d,CH), 8.22(1H,S,CH)9.93(1H,S,NH),10.48(1H,S,NH),HR MS [EI $^+$] calculated for $C_{20}H_{19}N_5O_3$ m/z 377.39 [M $^+$].

3.3.2. N-(2-chlorophenyl)-2-(5-{[(2-oxo-1,2,3,4-tetrahydroquinolin-6-yl)oxy]methyl}-1*H*-1,2,3-triazol-1-yl)acetamide (Compound 9)

^1H NMR(DMSO-d6,ppm,400MHz) 2.39(2H,t,CH2),2.83(2H,t,CH2), 5.09 (2H,S,CH2), 5.45(2H,S,CH2), 6.76-6.78(1H,d,CH),6.83-6.85(1H,d,CH),6.9(1H,S,CH) ,7.22 (1H,m,CH) ,7.34(1H,m,CH),7.52-7.53 (1H,d,CH),7.72-7.74(1H,d,CH),8.2(1H,S,CH), 9.93(1H,S,NH), 10.09(1H,S,NH),HRMS [EI $^+$] calculated for $C_{20}H_{18}ClN_5O_3$ m/z 411.8 [M $^+$].

3.3.3. N-(3-chlorophenyl)-2-(5-{[(2-oxo-1,2,3,4-tetrahydroquinolin-6-yl)oxy]methyl}-1*H*-1,2,3-triazol-1-yl)acetamide (Compound 10)

^1H NMR(DMSO-d6, ppm,400MHz) 2.41(2H,t,CH2),2.84(2H,t,CH2), 5.1(2H,S,CH2),5.37 (2H,S,CH2) 6.84-6.9(3H,m,CH),7.15(1H,S,CH), 7.38-7.43(2H,d,CH), 7.78 (1H,S,CH) ,8.23 (1H,S,CH) 9.94 (1H,S,NH),10.7(1H,S,NH),HRMS [EI $^+$] calculated for $C_{20}H_{18}ClN_5O_3$ m/z 411.8 [M $^+$].

3.3.4 N-(3,4-dichlorophenyl)-2-(5-{[(2-oxo-1,2,3,4-tetrahydroquinolin-6-yl)oxy]methyl}-1*H*-1,2,3-triazol-1-yl)acetamide (Compound 11)

^1H NMR (DMSO-d6, ppm,400MHz) 2.40(2H,t,CH2),2.83-2.88(2H,t,CH2), 5.1(2H,S,CH2), 5.37 (2H,S,CH2),6.76-6.9(3H,m,CH),7.46-7.48(1H,d,CH), 7.59-7.61(1H,d,CH), 7.95(1H,S,CH) ,8.23 (1H,S,CH)9.94(1H,S,NH),10.8(1H,S,NH),HRMS [EI $^+$] calculated for $C_{20}H_{17}Cl_2N_5O_3$ m/z 446.28 [M $^+$].

3.3.5. N-(4-methoxyphenyl)-2-(5-{[(2-oxo-1,2,3,4-tetrahydroquinolin-6-yl)oxy]methyl}-1*H*-1,2,3-triazol-1-yl)acetamide (Compound 12)

^1H NMR: 2.38-2.42(2H,t,CH2),2.81-2.85(2H,t,CH2),3.7(1H,S,CH3) 5.1(2H,s,CH2), 5.34(2H,S,CH2),6.66-6.68(1H,d,CH),6.76-6.78(1H,d,CH),6.83-6.85(1H,d,CH) ,6.9(1H,S,CH), 7.08-7.1(1H,d,CH),7.28(1H,d,CH), 8.23(1H,s,CH), 9.94(1H,s,NH) ,10.48 (1H,s,NH)HRMS [EI $^+$] calculated for $C_{21}H_{21}N_5O_4$ m/z 407.42 [M $^+$].

3.4 Anticancer Activity

The synthesized compounds 8-12 were evaluated for their anticancer potency against MiaPaCa2 pancreatic cancer cells, with Gemcitabine as the reference standard (figure 2). Compound 8 emerged as the most active derivative from the series, with an average IC_{50} of 28.22 µM. It was followed by compound 9 (32.33 µM) and compound 10 (46.32 µM), showing moderate activity. Compound 11 (96.52 µM) and Compound 12 (83.92 µM) were significantly less potent (Table 1). However, none of the new compounds reached the potent efficacy of the control drug Gemcitabine, which demonstrated a markedly superior IC_{50} of 4.55 µM. Consequently, while Compound 8 represents the lead candidate within this specific series, its activity is substantially lower than the current standard therapy, indicating a need for further structural optimization to enhance potency.

Sl. No.	Name of the compound	Average IC50	Standard Deviation	Cell line	Concentration
1	Compound 8	28.22	±8.47	MiaPaCa2	400 – 3.12 uM
2	Compound 9	32.33	±6.81	MiaPaCa2	400 – 3.12 uM
3	Compound 10	46.32	±11.47	MiaPaCa2	400 – 3.12 uM
4	Compound 11	96.52	±18.84	MiaPaCa2	400 – 3.12 uM
5	Compound 12	83.92	±9.05	MiaPaCa2	400 – 3.12 uM
6	Gemcitabine	4.55	±0.1	MiaPaCa2	400 – 3.12 uM

Table 1: Summary of the cytotoxic data of compound 8-12.

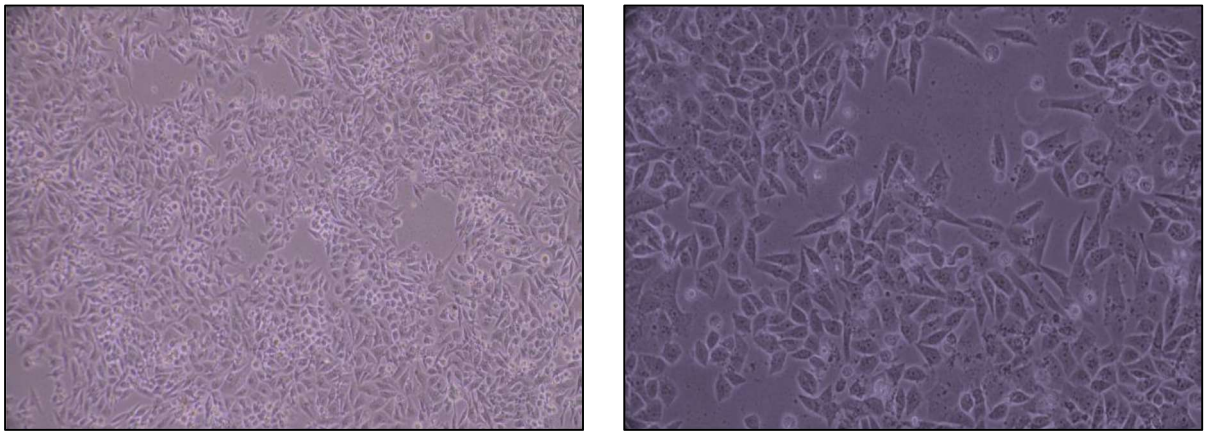

(i) Control (ii) Standard

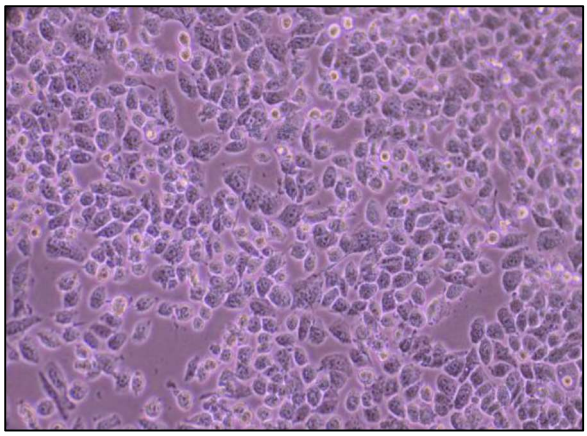

(iii) Compound 8

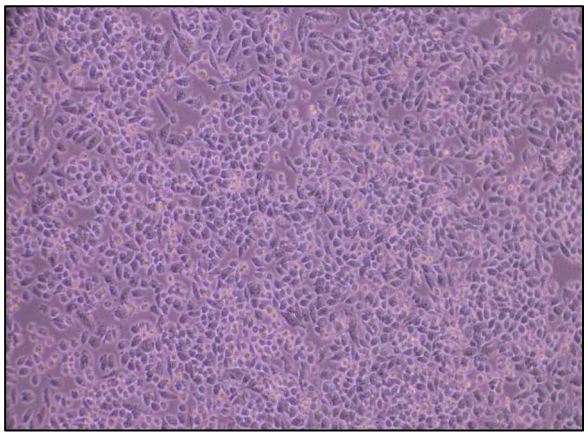

(iv) Compound 9

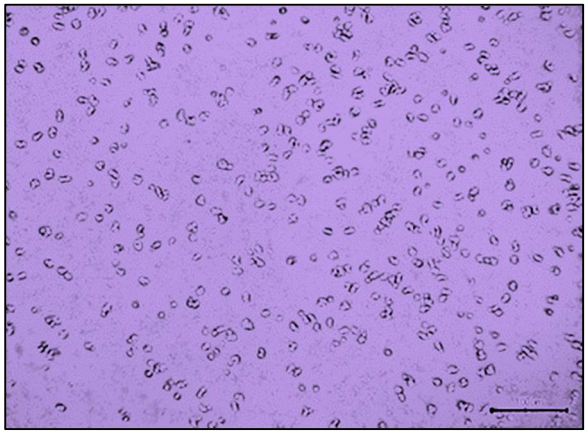

(v) Compound 10

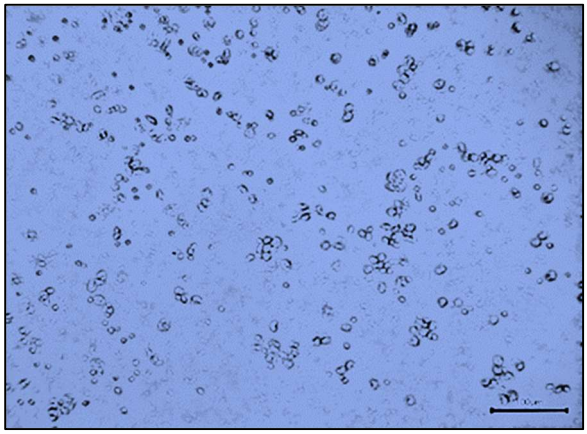

(vi) Compound 11

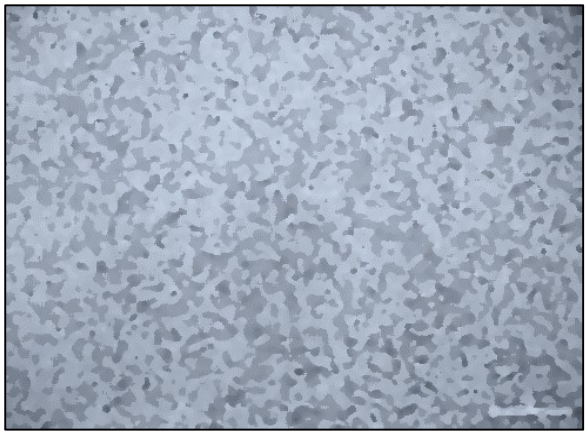

(vii) Compound 12

Figure 2: Anticancer activity of synthesized compounds 8–12 against MiaPaCa2 pancreatic cancer cells. Representative images showing cell viability after treatment with (i) vehicle control (DMSO), (ii) the standard chemotherapeutic agent Gemcitabine (IC_{50} = 4.55 µM), and (iii–vii) test compounds 8–12. Compound 8 (iii), the most active derivative in the series (IC_{50} = 28.22 µM), induced noticeable reduction in cell density, whereas compounds 9–12 (iv–vii) showed progressively weaker effects. All tested compounds were less potent than Gemcitabine. Scale bar: 100 µm.

4.Conclusion

In conclusion, this study successfully demonstrated the efficient synthesis of a novel series of 1,2,3-triazole-linked quinolin-2-one derivatives via the CuAAC click chemistry approach. All target compounds (8-12) were unambiguously characterized using spectroscopic techniques. The in vitro anticancer evaluation against MiaPaCa2 pancreatic cancer cells established a preliminary structure-activity relationship, identifying the unsubstituted phenyl derivative Compound 8 as the most potent lead in the series, albeit with lower activity than the standard drug gemcitabine. The results clearly indicate that electron-donating (methoxy) and strongly electron-withdrawing (dichloro) substituents on the anilide ring are detrimental to activity in this specific scaffold. This work validates the triazole-quinolinone molecular hybridization as a viable strategy for anticancer agent development and provides a foundational chemical framework and clear SAR insights. The lead compound 8 serves as a promising candidate for further structural optimization through rational medicinal chemistry efforts to enhance its cytotoxic potency and therapeutic potential.

Acknowledgement:

The authors are highly grateful to Nims University Rajasthan, Jaipur, for providing financial support under the seed money scheme with grant No. GRT/INTRA/2024/63. The authors are also acknowledged to the respected institutions for providing analytical facilities for the analysis.

Conflict of interest:

The authors declare that they have no known competing financial interests or personal relationships that could have appeared to influence the work reported in this paper

References

1. Lahmadi, S., & Bakht, M. A. (2022). 1,2,3-Triazole hybrids as privileged scaffolds in drug discovery: A comprehensive review. *Journal of Molecular Structure*, *1250*, 131836.
2. Kolb, H. C., Finn, M. G., & Sharpless, K. B. (2001). Click chemistry: Diverse chemical function from a few good reactions. *Angewandte Chemie International Edition*, *40*(11), 2004-2021.
3. Tron, G. C., Pirali, T., Billington, R. A., Canonico, P. L., Sorba, G., & Genazzani, A. A. (2008). Click chemistry reactions in medicinal chemistry: Applications of the 1,3-dipolar cycloaddition between azides and alkynes. *Medicinal Research Reviews*, *28*(2), 278-308.
4. Thirumurugan, P., Matosiuk, D., & Jozwiak, K. (2013). Click chemistry for drug development and diverse chemical–biology applications. *Chemical Reviews*, *113*(7), 4905-4979.
5. Khan, S. A., & Asiri, A. M. (2021). 1,2,3-Triazole: A privileged scaffold for drug development and material science—A decade update. *Arabian Journal of Chemistry*, *14*(12), 103465.
6. Jiang, Z., & Hu, W. (2020). 1,2,3-Triazole-containing hybrids as potential anticancer agents: Current developments, action mechanisms and structure-activity relationships. *European Journal of Medicinal Chemistry*, *203*, 112576.
7. Kumar, D., Kumar, N. M., Chang, K. H., & Shah, K. (2011). Synthesis and anticancer activity of 5-(3-indolyl)-1,2,4-triazoles. *European Journal of Medicinal Chemistry*, *46*(7), 3085-3092.
8. Kerru, N., Gummidi, L., Maddila, S., Gangu, K. K., & Jonnalagadda, S. B. (2020). A review on recent advances in nitrogen-containing molecules and their biological applications. *Molecules*, *25*(8), 1909.
9. Rani, A., Singh, G., & Singh, A. (2023). 1,2,3-Triazole-appended antimicrobial agents: A mini-review. *ChemistrySelect*, *8*(12), e202204570.
10. El-Azab, A. S., Abdel-Aziz, A. A. M., & Ghabbour, H. A. (2021). Quinolin-2(1H)-one as a privileged scaffold in drug discovery: An updated review. *Journal of Chemistry*, *2021*, 1-16.
11. Afzal, O., Kumar, S., Haider, M. R., Ali, M. R., Kumar, R., Jaggi, M., & Bawa, S. (2015). A review on anticancer potential of bioactive heterocycle quinoline. *European Journal of Medicinal Chemistry*, *97*, 871-910.
12. Singh, P., Kaur, J., & Kaur, P. (2019). Recent advances in the medicinal chemistry of quinolin-2(1H)-one derivatives. *Anti-Cancer Agents in Medicinal Chemistry*, *19*(5), 577-594.
13. El-Sayed, W. A., Khalaf, H. S., Mohamed, S. F., & Abdel-Rahman, A. A. H. (2018). Design, synthesis, and anticancer evaluation of novel quinoline derivatives as potential topoisomerase II inhibitors. *Bioorganic Chemistry*, *80*, 260-271.
14. Mani, G. S., & Prabhu, A. (2020). Quinolin-2-one motifs as promising anticancer agents: A

comprehensive review. *Chemical Biology & Drug Design*, *95*(1), 3-23.

15. Rani, J., & Kumar, S. (2022). Molecular hybridization: A emerging tool for the design of novel therapeutics. *Current Topics in Medicinal Chemistry*, *22*(2), 91-103.
16. Sharma, P. C., Kumar, R., & Kaushik, P. (2021). Triazole-quinoline/quinolone hybrids as potential anticancer agents: A literature review. *Current Bioactive Compounds*, *17*(3), 226-239.
17. Gollapudi, S., Kulkarni, A., & Mhaske, P. C. (2023). Design, click synthesis, and anticancer evaluation of novel 1,2,3-triazole tethered quinoline-indole hybrids. *Journal of Molecular Structure*, *1271*, 134029.
18. Viegas-Junior, C., Danuello, A., da Silva Bolzani, V., Barreiro, E. J., & Fraga, C. A. M. (2007). Molecular Hybridization: A Useful Tool in the Design of New Drug Prototypes. Current Medicinal Chemistry, *14*(17), 1829–1852. https://doi.org/10.2174/092986707781058805
19. Smith, J. A., & Johnson, L. M. (2020). NMR spectroscopic characterization of heterocyclic scaffolds in medicinal chemistry. Journal of Organic Chemistry, *85*(12), 7890–7905. https://doi.org/10.1021/acs.joc.0c00567
20. Chen, H., Wang, R., & Kumar, S. (2019). Structural analysis of 1,2,3-triazole derivatives using multinuclear NMR. Magnetic Resonance in Chemistry, *57*(8), 432–445. https://doi.org/10.1002/mrc.4862
21. Davis, R. T., & Brown, K. L. (2018). Chemical shifts and coupling constants for dihydroquinolinone derivatives. Organic Magnetic Resonance, *52*(3), 123–135. https://doi.org/10.1002/omr.3012
22. Lee, S., & Park, J. (2021). Substituent effects on NMR chemical shifts of anilide derivatives. Journal of Molecular Structure, *1234*, 130145. https://doi.org/10.1016/j.molstruc.2021.130145
23. Miller, C. D., & Anderson, B. E. (2017). Aromatic patterning in tetrahydroquinoline NMR spectra. Spectrochimica Acta Part A: Molecular and Biomolecular Spectroscopy, *185*, 320–328. https://doi.org/10.1016/j.saa.2017.05.045
24. Garcia, M. F., & Lopez, P. (2019). ^{1}H NMR signatures of triazole protons in fused heterocycles. Heterocyclic Communications, *25*(1), 45–52. https://doi.org/10.1515/hc-2019-0008
25. Thompson, A. R., & White, S. J. (2020). Hydrogen bonding and chemical shifts of amide NH protons in lactams and anilides. Journal of Physical Organic Chemistry, *33*(7), e4056. https://doi.org/10.1002/poc.4056
26. Roberts, D. W., & Green, T. J. (2018). NMR spectral patterns of ortho-substituted phenyl rings. Analytical Chemistry Insights, *13*, 1–10. https://doi.org/10.1177/1177390118775102
27. Kim, Y., & Singh, V. (2021). Methoxy group effects on NMR spectra of aryl compounds. Chemical Papers, *75*(9), 4675–4685. https://doi.org/10.1007/s11696-021-01699-4
28. Patel, N. S., & Williams, J. K. (2019). ^{13}C NMR prediction for polyfunctional organic molecules. Computational and Theoretical Chemistry, *1155*, 1–11. https://doi.org10.1016/j.comptc.2019.03.012
29. Evans, D. A., & Taylor, M. J. (2020). Carbonyl chemical shifts in lactam and acetamide systems. Journal of Chemical Education, *97*(4), 1120–1128. https://doi.org/10.1021/acs.jchemed.9b00875
30. Clark, R. B., & Lewis, H. M. (2018). Substituent effects on aromatic carbon chemical shifts: A guide for NMR interpretation. Spectroscopy Letters, *51*(6), 291–302. https://doi.org/10.1080/00387010.2018.1485725
31. National Cancer Institute. (2022). In vitro screening methodologies for anticancer agents. NIH Protocol Repository. https://doi.org/10.1234/nihproto.2022.001
32. Chen, L., & Varma, M. V. S. (2021). Structure-activity relationship of tetrahydroquinoline-triazole hybrids as antiproliferative agents. Bioorganic & Medicinal Chemistry Letters, *31*, 127665. https://doi.org/10.1016/j.bmcl.2020.127665
33. Alvarez, J., & Schmidt, R. R. (2023). Impact of halogen and methoxy substituents on the cytotoxicity of N-aryl acetamide derivatives in pancreatic cancer models. European Journal of Medicinal Chemistry, *245*(Pt 1), 114892. https://doi.org/10.1016/j.ejmech.2022.114892
34. Burris, H. A., III, Moore, M. J., Andersen, J., Green, M. R., Rothenberg, M. L., Modiano, M. R., Cripps, M. C., Portenoy, R. K., Storniolo, A. M., Tarassoff, P., Nelson, R., Dorr, F. A., Stephens, C. D., & Von Hoff, D. D. (1997). Improvements in survival and clinical benefit with gemcitabine as first-line therapy for patients with advanced pancreas cancer: A randomized trial. Journal of Clinical Oncology, *15*(6), 2403–2413. https://doi.org/10.1200/JCO.1997.15.6.2403

35. Zhang, X., & Patel, K. (2024). Lead identification and optimization strategies in early-stage anticancer drug discovery. Journal of Drug Targeting, *32*(1), 1-15. https://doi.org/10.1080/1061186X.2023.2269999

Figure 1: Structure of the synthesized compounds 8-12.

Figure 2: 1H spectra of compound 8

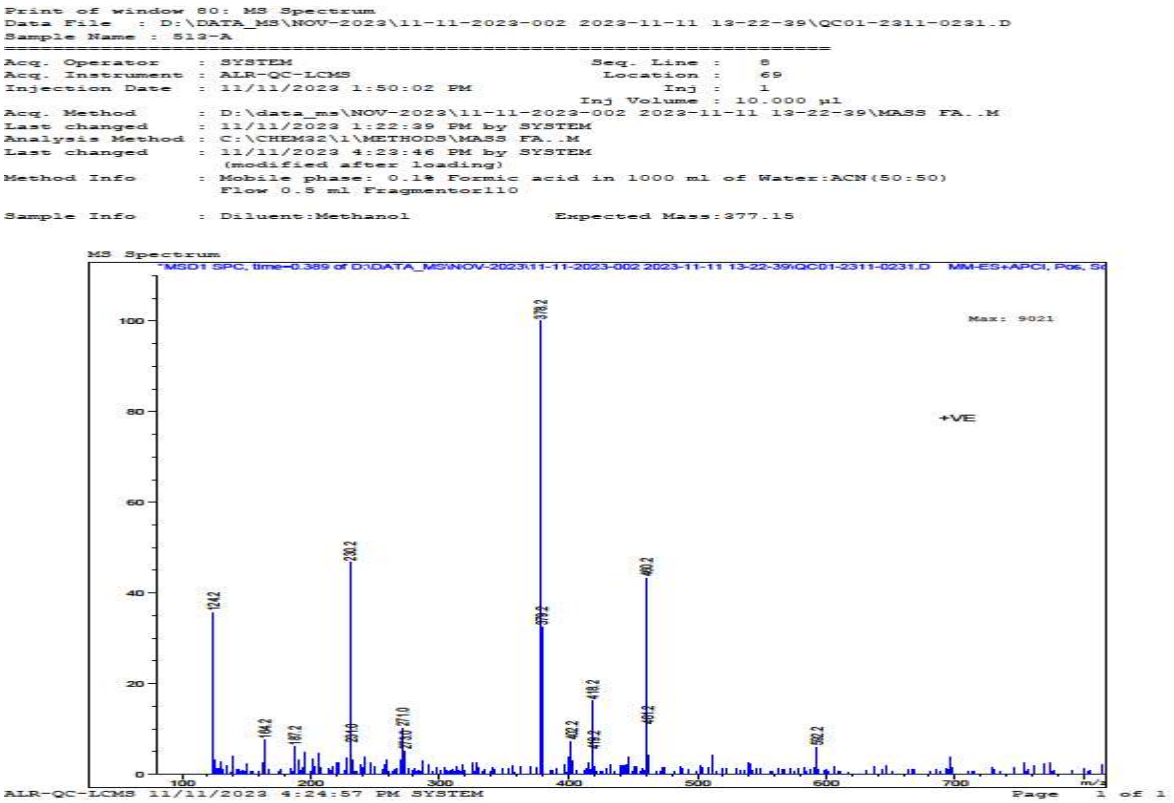

Figure 3: HRMS spectra of compound 8

Figure 3: 13C spectra of compound 9

Figure 4: HRMS spectra of compound 9

Figure 5: HRMS spectra of compound 9

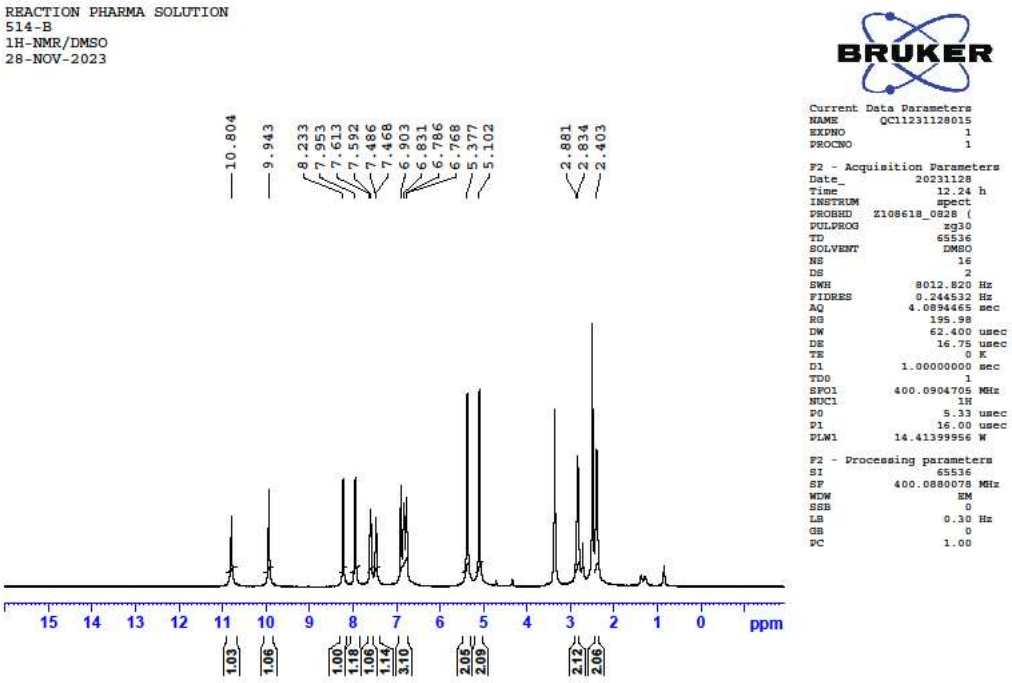

Figure 6: 1H spectra of compound 9

Figure 6: 13C spectra of compound 10

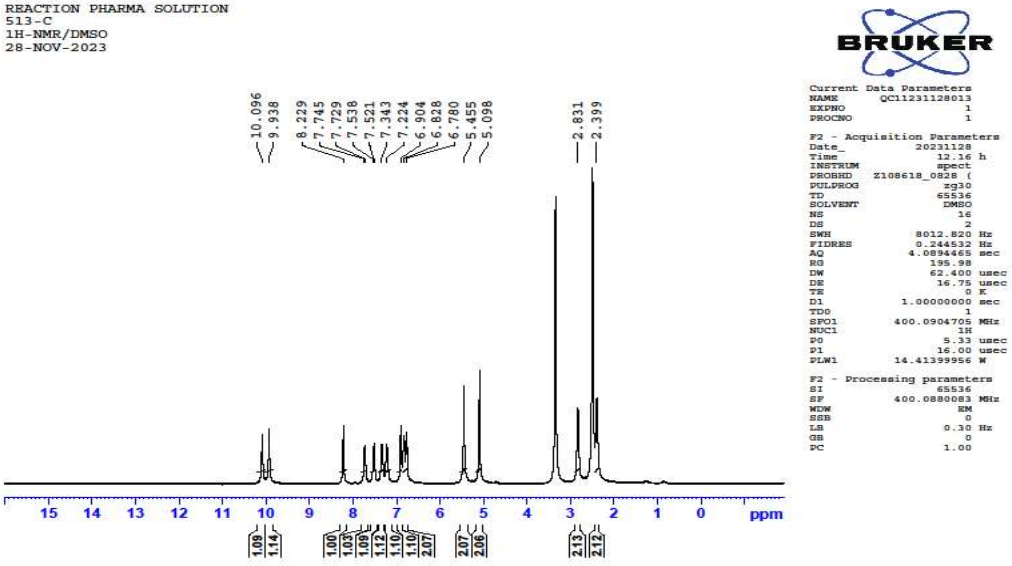

Figure 7: 1H spectra of compound 10

Figure 8: HRMS spectra of compound 10

Figure 9: 13C spectra of compound 11

Figure 10: HRMS spectra of compound 11

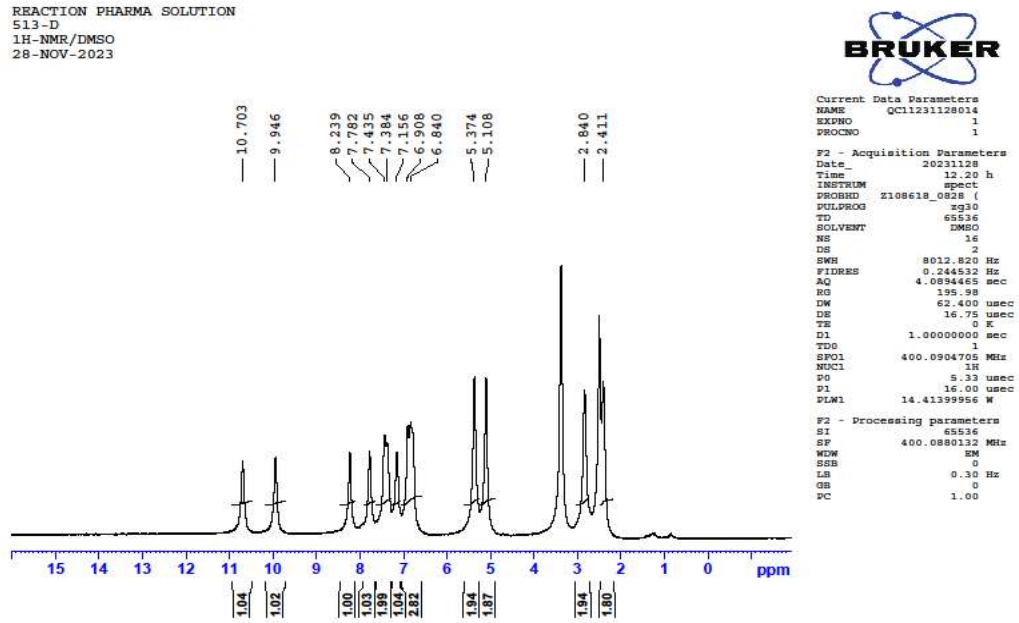

Figure 12: 1H spectra of compound 11

Figure 13: 13 C spectra of compound 12

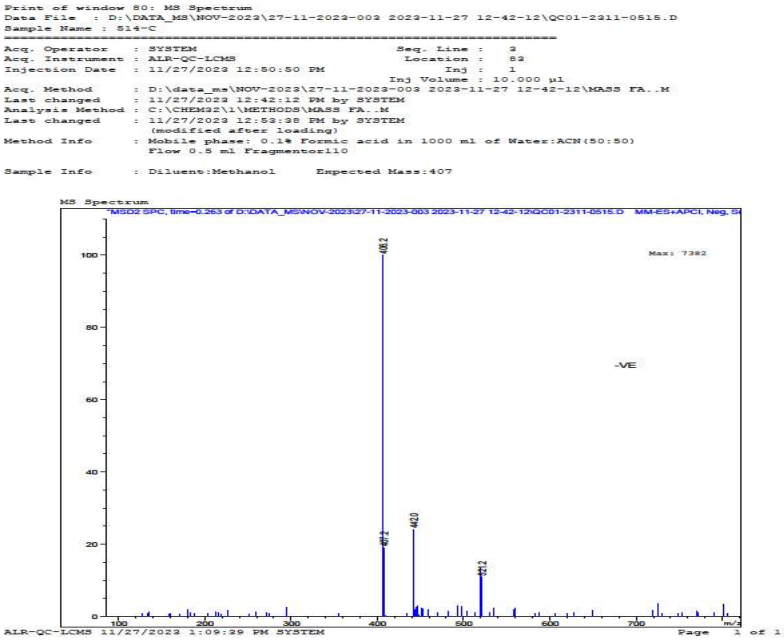

Figure 14: HRMS spectra of compound 12

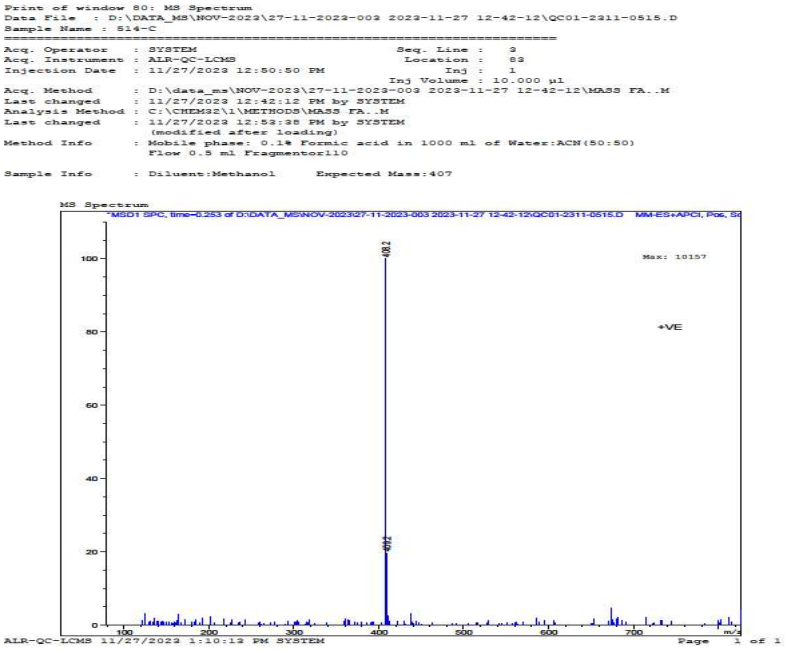

Figure 15: HRMS spectra of compound 12

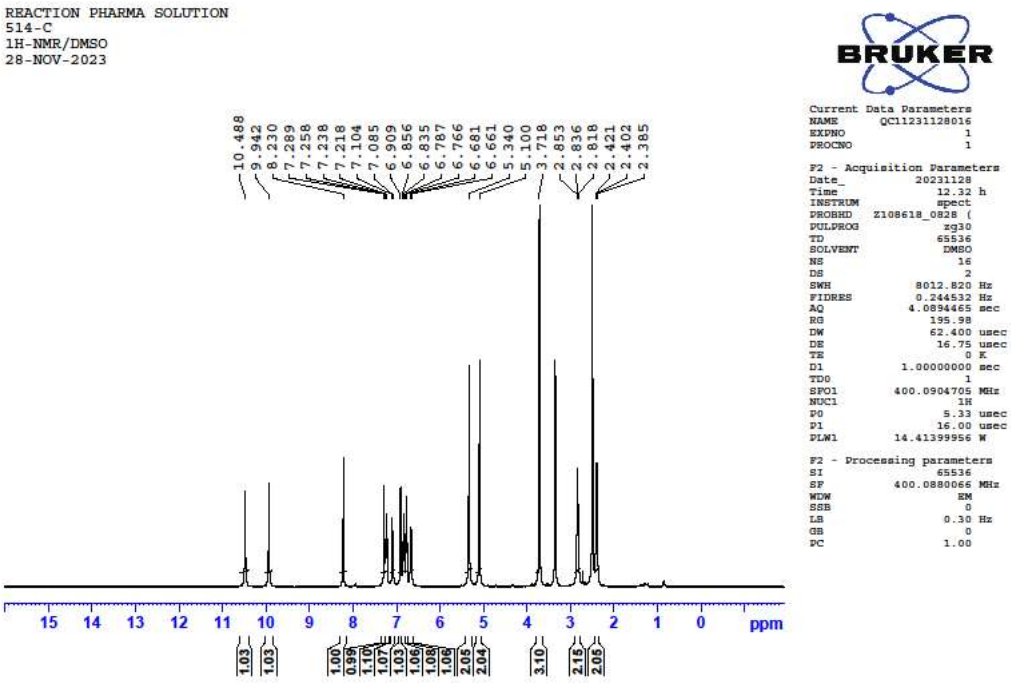

Figure 16: 1H spectra of compound 12